Journal of Statistical Physics, Vol. 66, Nos. 1/2, 1992

On Scaling Properties of Cluster Distributions in Ising Models

C. Ruge[1] and F. Wagner[1]

Received October 24, 1990; final July 9, 1991

Scaling relations of cluster distributions for the Wolff algorithm are derived. We found them to be well satisfied for the Ising model in $d=3$ dimensions. Using scaling and a parametrization of the cluster distribution, we determine the critical exponent $\beta/\nu = 0.516(6)$ with moderate effort in computing time.

KEY WORDS: $d=3$ Ising model; Wolff algorithm; cluster size distribution; critical exponents; finite-size scaling; parametrization.

1. INTRODUCTION

Local Monte Carlo simulations of Ising spin systems in the critical region are severely impaired be the so-called critical slowing down.[1,2] Cluster algorithms[3,4] improve this situation considerably. The transition from the disordered into the ordered phase of the system manifests itself by the onset of cluster percolation. If these clusters are physically relevant, the critical exponents describing the cluster distribution near the percolating threshold should be related to usual thermodynamic exponents. For the Swendsen–Wang algorithm[3] (hereafter called SWA), de Meo *et al.*[5] have suggested that the exponent in the power law of the cluster distribution near the critical temperature T_c is determined by the exponent β/ν. Obviously such a relation would be very useful, since cluster distributions can be measured at one value of the temperature and of the size L of the lattice. As one can see from the data of ref. 5 for the $d=2$ Ising model such a relation cannot hold at lattice sizes treated in that work. However, finite-size scaling for the distribution for large clusters can be valid and provide additional information about the critical exponents. Whereas SWA decomposes the whole

[1] Institut für Theoretische Physik und Sternwarte, Universität Kiel, D-2300 Kiel, Germany.

0022-4715/92/0100-0099$06.50/0

lattice into clusters, in the algorithm advocated by Wolff[4] (hereafter abbreviated WA) only one cluster is constructed in each Monte Carlo step. As shown by Tamayo *et al.*,[6] in this method the fraction of large clusters is enhanced by an order of magnitude as compared to SWA, providing a better sensitivity to possible scaling properties. Also, it may lead to a further reduction of critical slowing down, depending on the dimension.[6–8] In this paper we derive and test for WA the analogous scaling properties to SWA. The hope of extracting critical exponents for the $d=3$ Ising model from single cluster distributions turns out not to be justified, at least not within our statistics and the considered range of lattice size $L \leqslant 36$. One of the main objectives of this paper is to find a reasonable parametrization of the cluster distribution. If finite-size scaling is true, such a parametrization can be used for an accurate determination of the exponents involved in the scaling region.

The paper is organized as follows. Section 2 summarizes the cluster algorithm and the relation of the cluster distribution to the physical observables. In Section 3 we derive the exponents in a finite-size scaling law for clusters and present the motivation for the parametrization employed. Section 4 contains the comparison of scaling and parametrization with Monte Carlo simulations of the $d=3$ Ising model. In Section 5 we give our conclusions.

2. CLUSTER ALGORITHMS

We consider spin variables $\sigma_x = \pm 1$ defined on the sites of a d-dimensional cubic lattice of length L and volume $V = L^d$. An Ising model is characterized by the energy between next neighbors,

$$E(\sigma) = -\sum_{x,\mu} \sigma_x \sigma_{x+\mu} \tag{1}$$

The summation in (1) runs over all links $(x, x+\mu)$. We are interested in the expectation value of an observable A in thermodynamic equilibrium

$$\langle A \rangle = \frac{1}{Z} \sum_{\{\sigma_x\}} A(\sigma) e^{-E(\sigma)/T} \tag{2}$$

A possible constant in (1) can be absorbed in the temperature T in (2). With the Monte Carlo method[2] Eq. (2) is evaluated by generating a sequence of spin configurations $\{\sigma\}_n$ with relative frequency proportional to the Boltzmann factor

$$p(\{\sigma\}) \sim e^{-E(\sigma)/T} \tag{3}$$

We get an estimator for $\langle A \rangle$ by summing over all generated configurations

$$\langle A \rangle \simeq \frac{1}{N} \sum_{n=1}^{N} A(\{\sigma\}_n) \tag{4}$$

The error in (4) is given by $\Delta\langle A \rangle = (t_a/\sqrt{N})\,\Delta A$, where ΔA denotes the measured variance and t_a the autocorrelation time. For a local algorithm (heat-bath or Metropolis[1]) t_a at the critical temperature T_c increases strongly with L, preventing (so-called critical slowing down) the simulation of large critical lattices. Cluster algorithms lead to substantially smaller values of t_a. They have in common the following prescription for constructing the cluster. If point x belongs to the cluster, a neighboring point x', which does not already belong to the cluster, is included with probability

$$p(x' \in C) = \begin{cases} 0, & \sigma_x \neq \sigma_{x'} \\ 1 - \exp(-2/T), & \sigma_x = \sigma_{x'} \end{cases} \tag{5}$$

This procedure is repeated until all neighboring points do not belong to the cluster. Equation (5) was proposed by Coniglio and Klein[9] and Hu.[10] Swendsen and Wang[3] developed an algorithm by using the prescription (5) to decompose the entire lattice and chosing with equal probability ± 1 for the spin on each cluster. The equivalence with the random cluster model[11] was used in the proof that the temperature dependence of (5) leads to the Boltzmann distribution (3).

In the single cluster method of Wolff[4] the successive spin configurations $\{\sigma\}_{n+1}$ are obtained from the $\{\sigma\}_n$ by chosing a starting point x_0 at random, constructing one cluster according (5), and reversing all spins σ_x of this cluster.

A quantity easily measurable in the algorithm is the cluster size distribution $p(s)$, where s denotes the number of sites belonging to the cluster. There exists a close connection between the Wolff cluster method and the SWA method.[4,12] One always can interpret one Wolff cluster as one member of a complete SWA decomposition of the lattice. Therefore the probability $p(s)$ to construct a cluster of size s in WA must satisfy the relation

$$p(s)_{\mathrm{WA}} = s n(s)_{\mathrm{SWA}} \tag{6}$$

where $n(s)$ denotes the number of s-clusters per spin in SWA. The SWA can be interpreted as a problem of correlated percolation.[3,11] Due to the identity (6), we can use this interpretation also for the Wolff cluster.

In the following we are interested in he critical region. This region is characterized by small values of the parameter

$$\tau = 1 - T/T_c \tag{7}$$

and large cluster sizes s with finite values of $s|\tau|^{\theta_2}$. In the high-temperature phase ($\tau < 0$) we expect (e.g., refs. 13) from percolation for the infinite system a cluster distribution of the following form:

$$p(s) = s^{-1-\theta_1} F(s|\tau|^{\theta_2}) \tag{8}$$

where $F(t)$ is regular at $t = 0$ and strongly decreasing at $t \to \infty$. The power law for p obtained by an extrapolation to $\tau \to 0$ will be modified by finite-size corrections. In the low-temperature phase ($\tau > 0$) percolating clusters will appear. A parametrization of the form (8) (eventually with a different scaling function F and different exponents $\theta_{1,2}$) will describe only the finite clusters. In addition there will be a contribution of the infinite cluster.

Two observables can be obtained from the cluster size distribution: the susceptibility/spin χ above T_c and the order parameter m below T_c. They can be derived from the Green's function

$$G = L^{-d} \sum_{x,y} \langle \sigma_x \sigma_y \rangle \tag{9}$$

As shown in ref. 12, G can be expressed as the mean cluster size

$$G = \int ds\, sp(s) \tag{10}$$

For $T > T_c$, the rhs of (9) coincides with the susceptibility and one gets

$$\chi = \int ds\, sp(s) \tag{11}$$

Below T_c the rhs side of (9) diverges in the limit $L \to \infty$ according to

$$G = L^d(m^2 + O(L^{-d})) \tag{12}$$

due to the finite order parameter m. In (10) this divergence results from the contribution of the percolating cluster. If the lattice size is larger than the correlation length ($L > \xi \sim |\tau|^{-\nu}$), the cluster distribution consists of two parts. Small clusters representing the finite clusters are well separated from large clusters forming a narrow peak at $s = s_p$. These large clusters are caused by the percolating cluster of the infinite system. A peak reflects a uniform density of this cluster. The large clusters dominate the rhs of Eq. (10) and we obtain

$$G \simeq s_P \int_{s_0}^{\infty} p(s)\, ds \tag{13}$$

where s_0 has to be chosen somewhere in the gap between finite and percolating clusters. Since the probability to end in a percolating cluster is given by

$$\int_{s_0} ds\ p(s) = s_P L^{-d} \tag{14}$$

we obtain finally from Eqs. (12–14)

$$m = \int_{s_0}^{\infty} ds\ p(s) \tag{15}$$

Note that the relation (11) is an exact identity for $T > T_c$, whereas (15) holds only up to $O(L^{-d})$ terms and requires a prescription to separate the large clusters from $p(s)$. Expressions for χ in the case $T < T_c$ and $m(\tau)$ in the range $T > T_c$ can be found in ref. 5 for SWA clusters. Since these rely on specific properties of the SWA decomposition of the lattice, they have no correspondence in the Wolff algorithm.

3. FINITE-SIZE EFFECTS

In the critical regime, finite-size scaling laws are expected to hold. In the first part of this section we generalize the results of ref. 5 for SWA clusters to the case of WA. The main effect of a finite L will be the occurrence of percolating clusters also for $T > T_c$. In the second part we treat this effect by a suitable parametrization of the cluster distribution.

Finite-size scaling follows from the invariance of the free energy under the following rescaling of the size L, temperature τ, and a small magnetic field H:

$$L \to L' = \rho L \tag{16}$$

$$\tau \to \tau' = \rho^{-1/\nu} \tau \tag{17}$$

$$H \to H' = \rho^{\beta/\nu - d} H \tag{18}$$

The exponents of ρ in (17, 18) describe the anomalous dimensions of τ and H in the critical regime. Eliminating one of the variables with (16)–(18), one gets the following scaling laws[14] for the susceptibility and the magnetization at $H = 0$:

$$\chi(\tau, L) = |\tau|^{2\beta - \nu d} \bar{\chi}(z) \tag{19}$$

$$m(\tau, L) = \tau^{\beta} \bar{m}(z) \tag{20}$$

The independent functions $\bar{\chi}$ and $\bar{m}$ only depend on the scale-invariant combination $z = |\tau|^{\nu} L$. Equations (19) and (20) are eqivalent to the following anomalous dimensions for χ and m:

$$\chi \to \chi' = \rho^{d-2\beta/\nu} \chi \tag{21}$$

$$m \to m' = \rho^{-\beta/\nu} m \tag{22}$$

To derive the critical exponents in a scaling law for the cluster distribution, we have to know the anomalous dimension of s and the distribution function $p(s, \tau, L)$ for large s according to

$$s \to s' = \rho^{y_s} s \tag{23}$$

$$p \to p' = \rho^{y_p} p \tag{24}$$

For $T > T_c$ we can extend the limits of integration in (11) to the scale-invariant interval $[0, \infty]$, since near $s = 0$ we obtain for $\theta_1 < 1$ only a finite contribution to the divergent χ and at $s \to \infty$ the distribution $p(s)$ should vanish exponentially. The scaling dimensions on both sides of Eq. (11) have to match, which leads to

$$2y_s + y_p = d - \frac{2\beta}{\nu} \tag{25}$$

The same argument can be applied to Eq. (15), since for sufficiently small $T < T_c$ the order parameter m does not depend on s_0. Comparing the dimensions on both sides of Eq. (15), we obtain a second relation between y_s and y_p,

$$y_s + y_p = -\frac{\beta}{\nu} \tag{26}$$

Assuming the same diension below and above T_c, (25) and (26) fix the anomalous dimension of s and p under the transformation (16),

$$s \to s' = \rho^{d-\beta/\nu} s \tag{27}$$

$$p \to p' = \rho^{-d} p \tag{28}$$

From (27), we see that the cluster density $x = sL^{-d}$ has the dimension of a magnetization, and from (28), pL^d has to be dimensionless. Substituting the density x for the cluster size s, we see that the corresponding distribution function $q(x, \tau, L)$ must be scale invariant. It can only depend on two of the combinations $y = x(L/L_0)^{\beta/\nu}$, $y' = x|\tau|^{-\beta}$, and $z = |\tau|^{\nu} L$:

$$q(x, \tau, L) = \begin{cases} \bar{q}(x|\tau|^{-\beta}, z) \\ \bar{\bar{q}}(x(L/L_0)^{\beta/\nu}, z) \end{cases} \tag{29}$$

The scale invariance of the distribution q of the cluster density $x = sL^{-d}$ appears to be less surprising, if we recall that for uncorrelated percolation $\int dx/x\, q(x)$ has the meaning of a free energy.[11,15] If the simple distribution (8) is valid, scaling requires for the exponents

$$\begin{aligned} \theta_1 &= 1/\delta \qquad \text{with} \quad \delta = \nu d/\beta - 1 \\ \theta_2 &= \nu d - \beta \end{aligned} \tag{30}$$

The scaling law (29) and the exponents (27), (28), (30) agree with those of ref. 5 for SWA clusters. As pointed out in ref. 5, the scaling functions may be more complicated. As a consequence, the exponent θ_1 at $\tau \neq 0$ may not agree with (30), whereas (29) still holds. Equation (29) allows a test of scaling without resorting to a particular parametrization such as (8) by plotting the cluster distribution q at a fixed value of z as a function of $y = (L/L_0)^{\beta/\nu}$ or $y' = x|\tau|^{-\beta}$. If (29) is true, the distributions should be independent of L. A more accurate test of scaling is possible if we use a parametrization of the cluster distribution. A form motivated by the Fisher droplet model[16]

$$q_1(x) = \frac{c}{x^{1+\theta_1}} \exp^{-(\lambda x)^{\theta_3}} \tag{31}$$

describes the data only for $T > T_c$ and large sizes L with $\theta_3 = 1$. We get finite-size corrections by the following consideration. The WA generates clusters locally and therefore we expect all large clusters to have the same average density. At a finite volume there will be a critical density μ, where clusters of the infinite system with $s > \mu L^d$ are prevented from any further growth. This leads to the following modification of (31):

$$q(x) = q_1(x)\, \theta(\mu - x) + c_P\, \delta(x - \mu) \tag{32}$$

The critical density μ will fluctuate and by this the discontinuous function (32) will be turned into a smooth curve. A simple Gauss distribution for μ will not be adequate, since fluctuations larger than the mean value are still cut off by the finite size, whereas smaller ones are not. Therefore we use an asymmetric Gaussian defined as

$$g(t, r) = \frac{1}{(2\pi)^{1/2}} \left(\theta(t) e^{-t^2/2(1+r)^2} + \theta(-t) e^{-t^2/2(1-r)^2}\right) \tag{33}$$

and replace the δ function in (32) by $g((x-\mu)/\sigma, r)/\sigma$ with a finite width σ. We have a width $\sigma(1+r)$ for $x < \mu$ and $\sigma(1-r)$ for $x > \mu$. In the same

way the step function is replaced by the analogous complementary error function

$$E(t, r) = \int_t^\infty dt'\, g(t', r) \tag{34}$$

For $T < T_c$ the exponent θ_3 in (31) should be $1 - 1/d$. This is pure geometrical effect of SWA clusters, that formation of finite clusters in the presence of the percolating cluster is suppressed by the physical surface.[15] Because of (6), this also holds for the WA clusters. Therefore (32) should be applied to the data in the form

$$q_2(x) = \frac{c}{x^{1+\theta_1}} \exp^{-(\lambda x)^{\theta_3}} E\left(\frac{x-\mu}{\sigma}, r\right) + \frac{c_P}{\sigma} g\left(\frac{x-\mu}{\sigma}, r\right) \tag{35}$$

with

$$\theta_3 = \begin{cases} 1, & T > T_c \\ 1 - 1/d, & T < T_c \end{cases} \tag{36}$$

Equation (31) may be recovered from (36) by putting $\mu = \infty$. We use both forms only as a parametrization. In particular, the exponent θ_1 may differ from its scaling value $1/\delta$ from Eq. (30) if the scaling function $\bar{q}$ or $\bar{\bar{q}}$ is a more complicated function of its two arguments. At $\tau = 0$, $q(x, 0, L)$ is a function of y only. We can use (35) as a parametrization of the scaling function

$$q_3(x) = c y^{\nu d/(\beta - \nu d)} \exp^{-(\lambda y)^{1-1/d}} E\left(\frac{y-\mu}{\sigma}, r\right) + \frac{c_P}{\sigma} g\left(\frac{y-\mu}{\sigma}, r\right)$$
$$\text{with} \quad y := x\left(\frac{L}{L_0}\right)^{\beta/\nu} \quad \text{and} \quad L_0 = 20 \tag{37}$$

The choice of the exponent $\theta_3 = 1 - 1/d$ is motivated by the fact that the finite system at $\tau = 0$ already exhibits a percolating cluster. Note that if scaling is true, the parameters μ, σ in (35) should scale like a magnetization, whereas in (37) this dependence is already taken into account by the L dependence of y.

In the next section we compare the parametrization $q_{1,2,3}$ in Eqs. (31), (35), and (37) with Monte Carlo simulations of the $d = 3$ Ising model.

4. COMPARISON WITH THE $d = 3$ ISING MODEL

To compare the scaling properties of the cluster distribution with MC simulation, we prefer $d = 3$ over $d = 2$ for several reasons. In $d = 2$ thermal

quantities at $H=0$ and critical indices are known exactly. Moreover, the percolation point for geometrical clusters should coincide with the thermal critical point for topological reasons.[15] Also, there already exists a study of the Swendsen–Wang cluster method for $d=2$.[5] To perform the comparisons mentioned at the end of Section 3, the critical temperature and partly the exponents have to be known, which have been determined for $d=3$ (s.c. lattice) with high accuracy by Pawley *et al.*[17]:

$$\frac{1}{T_c}=0.221655(4) \tag{38}$$

$$\nu=0.629(4) \tag{39}$$

$$\beta=0.324(4) \tag{40}$$

$$\delta=\frac{\nu d}{\beta}-1=4.83(3) \tag{41}$$

These values agree within errors with those obtained in refs. 18 and 19 and the values obtained by series expansion.[20] $\tau=(T-T_c)/T_c$ always refers to (38). The values of ν, β, and δ are taken from (39)–(41) whenever we refer in the following to known values of the exponents. We simulated the $d=3$ Ising model (1) at various τ with the WA on simple cubic lattices of size L ($12\leqslant L\leqslant 36$) with periodic boundary conditions. To identify percolating clusters on a finite volume we made one run ($L=20$, $\tau=0$) with cylinder geometry (free boundary conditions in one direction and periodic in the others). We used mainly data for $T\geqslant T_c$, since for $T<T_c$ also WA becomes inefficient and within our assumption of equal critical behavior above and below T_c we cannot learn anything more about critical indices. Typically we generated 10^4–10^5 clusters at each set of values of τ and L, from which we determined the distribution $q(x, \tau, L)$. Statistical errors are obtained by binning the data and taking $\Delta q_x=1/\sqrt{N_x}$ in each bin. A bin size exponentially increasing with x accounts for the decrease of q over 6–7 orders of magnitude from $x=1/L^d$ to $x\sim O(1)$. Our errors are purely statistical and do not include the autocorrelation time $t_a(x)$, which ought to have been determined for each x separately. We can estimate an average value from the susceptibility $\chi=\int dx\, xq(x)$, which leads to $t_a\sim 2$–4, depending on τ and L.

Figure 1 shows $q(x)$ for $T>T_c$ at $\tau=-0.054$ and $L=20$ on a double logarithmic scale. $z=3.19$ is sufficiently large that the power law is cut off by the exponential factor in (31) before finite-size corrections can become important. The curve is a fit with the parametrization (31). The parameter values for λ, θ_1, c are obtained by minimizing χ^2 and are given in Table I

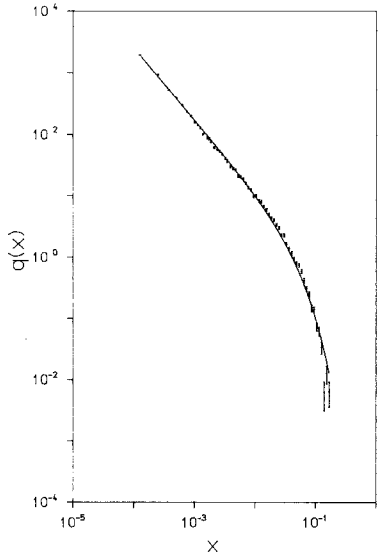

Fig. 1. Measured cluster distribution $q(x)$ for $T > T_c$ at $\tau = -0.054$ and $L = 20$ ($z = 3.19$) as a function of x on a double logarithmic scale. The curve is a fit using (31). Parameters are given in Table I, Fit A.

Table I. Parameters for the Various Fits Performed[a]

	Fit A	Fit B	Fit C	Fit D	Fit E
# (clusters)	5×10^4	6×10^4	6×10^5	8×10^5	2×10^4
τ	-0.054	-0.0066	0	0	0.060
L	20	28	20, 28, 36	20(cyl.)	20
z	3.19	1.1	0	0	3.41
Equation	(31)	(35)	(37)	(35)	(35)
χ^2/N_{data}	296/60	66/60	1550/195	928/70	73/45
c	0.058(2)	0.0242(2)	0.0255(6)	0.0324(5)	0.030(4)
λ	21.5(8)	0.3(3)	9.7(3)	1.8(1)	61(2)
θ_1	0.157(3)	0.208	0.208	0.224(3)	0.220(3)
θ_3	1	1	2/3	2/3	2/3
μ	∞	0.187(6)	0.3441(5)	0.213(2)	0.556(5)
σ	—	0.076(1)	0.0902(5)	0.108(9)	0.030(1)
r	—	0.43(3)	0.446(3)	0.407(40)	0.027(2)
c_P	0	0.42(5)	0.645(3)	0.555(20)	0.97(1)

[a] The first line gives the number of cluster Monte Carlo steps. Line 5 identifies the used parametrization by the number of the equation. Line 6 indicates the χ^2 obtained for N_{data} points used in the fit, and in the remaining lines the parameter values are listed. Errors in parentheses refer to units of the last figure given and do not include t_a. Entries without errors are kept fixed in the fit.

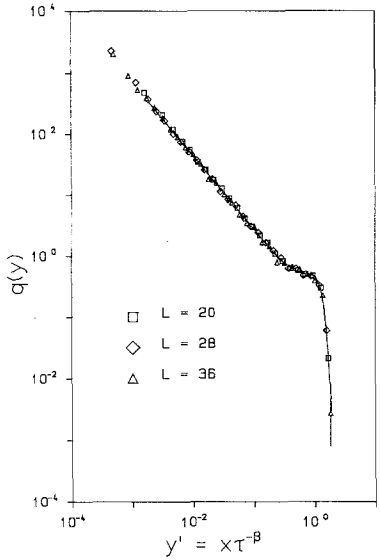

Fig. 2. Measured cluster distribution q at $z=1.1$ for $T>T_c$ as a function of $x\tau^{-\beta}$ on a double log scale. Scaling is satisfied if the values at $L=20$ (□), $L=28$ (◇), and $L=36$ (△) coincide. The curve is a fit using (35) to the $L=28$ data for $s\geqslant 15$. Parameters in Table I, Fit B.

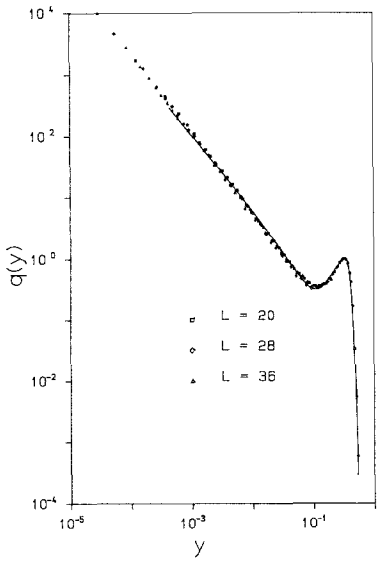

Fig. 3. Measured cluster distribution q at $z=0$ for $L=20$ (□), $L=28$ (◇), and $L=36$ (△) as a function of $y=xL^{\beta/\nu}$. The curve is to all data using (37), omitting clusters with $s\leqslant 15$. Parameters in Table I, Fit C. Scaling is satisfied if data for different L lie on the same curve.

(Fit A). We obtain a reasonable description of the data; however, the value $\theta_1 = 0.157(3)$ is in disagreement with $\theta_1 = 1/\delta = 0.208$ from (41). This low value of θ_1 depends entirely on the values of $q(x)$ at $s \leqslant 10$, where we neither expect (31) to be valid nor any scaling properties to hold. Omitting the low-s points, the fit can no longer separate a power law from an exponential decrease in his limited range of x. Decreasing τ, we find that finite-size corrections described by the Gaussian in (35) become important. This can be seen in Fig. 2, where the distributions at fixed $z = |\tau|^{\nu} L = 1.1$ are shown for various L as a function of $y' = x|\tau|^{-\beta}$. For β and ν we use the values (39), (40). From the agreement of the distributions for different L we conclude that the scaling law (29) is in good agreement with the data. The curve represents a fit using the parametrization (35) with $\theta_1 = 1/\delta$ and $\theta_3 = 1$ at $L = 28$. The parameter values are given in Table I (Fit B). The form (35) fits the transition to the contribution of the large, presumably percolating cluster extremely well. The value of $\chi^2 = 66$ for 60 data points is acceptable, bearing in mind that the errors do not include t_a. From the fit we excluded all points with $s \leqslant 15$. Otherwise the exponent θ_1 could not be kept at its scaling value. A test of scaling analogous to Fig. 2 for the $d = 2$ Ising model has been done in ref. 5 by separating the SWA cluster distribution $n(s)$ into the contribution of the largest cluster and the

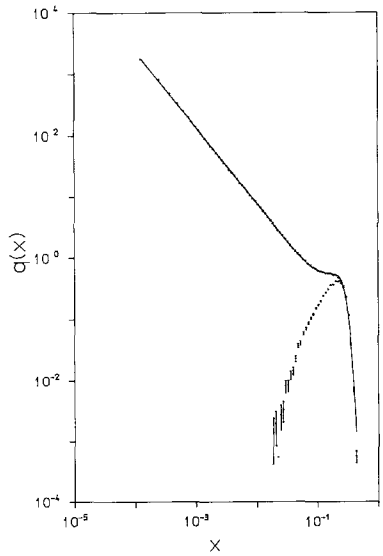

Fig. 4. Measured cluster distribution (dots) at $\tau = 0$ and $L = 20$ using film geometry. Open points represent the percolating clusters. The curve is obtained by a fit using the parametrization (37). Parameters in Table I, Fit D.

remainder. Since no errors have been given, it remains inconclusive whether the small deviations from scaling are due to statistical fluctuations or the separation mentioned before.

At the critical point $\tau = 0$ the finite-size corrections should become more prominent, which is indeed the case, as Fig. 3 shows. There we present the distribution q at $\tau = 0$ as a function of $y = x(L/L_0)^{\beta/\nu}$, taking β/ν from (39), (40) and $L_0 = 20$. If scaling (29) holds, q can only depend on y and distributions with different L should lie on the same curve. Again the scaling law (29) is well satisfied. The curve corresponds to a fit, using the parametrization (37), to all data with $s \geqslant 15$ (parameters given in Table I, Fit C).

To check that the Gaussian peak is due to the percolating clusters, we present in Fig. 4 the distribution at $\tau = 0$ and $L = 20 = L_0$ with cylinder geometry together with the clusters connecting the free surfaces of the lattice (open points). The curve represents a fit (Fit D in Table I) using (37), which, at $L_0 = 20$, is identical to (35). The Gaussian peak is dominated by the percolating cluster, as we would expect. Comparing the distributions in Figs. 3 and 4 or the values of the parameters in Table I, we see that the cluster properties are very sensitive to a change of boundary conditions. The fraction of 10% surface points suppresses the large clusters considerably.

In the fits to Fig. 2 and 3 we kept the exponent θ_1 at its scaling value. It cannot be reliably determined by a fit to a single x distribution, since a small change in the choice of $F(x)$ will have drastic effects on the value of θ_1. Nevertheless, the scaling laws (29) are very sensitive to the values of β and β/ν. At $z = 0$ only β/ν enters and the scaling value of $\theta_1 = \beta/\nu d - \beta$ depends on he same combination of exponents. If we repeat the fit in Fig. 3 with different values of β/ν, we can determine $\chi^2(\beta/\nu)$ as shown in Fig. 5. The minimum gives the best scaling exponent for our data. An error for β/ν can be determined by increasing χ^2 by the autocorrelation time t_a. Estimating the latter from the susceptibility, we should use the criterion $\Delta\chi^2 = 4$, leading to

$$\frac{\beta}{\nu} = 0.516(6) \tag{42}$$

Equation (42) is in agreement with $\beta/\nu = 0.51(1)$ using finite-size scaling of the susceptibility[19] and with 0.516(3) from Monte Carlo renormalization group methods[17] based on a local Metropolis method. Note that the cluster method requires substantially less effort in computing time to reach the same accuracy [knowing T_c, the data used for (42) require 15 hr on a VAX 8550 computer]. Determination of exponents from the scaling at

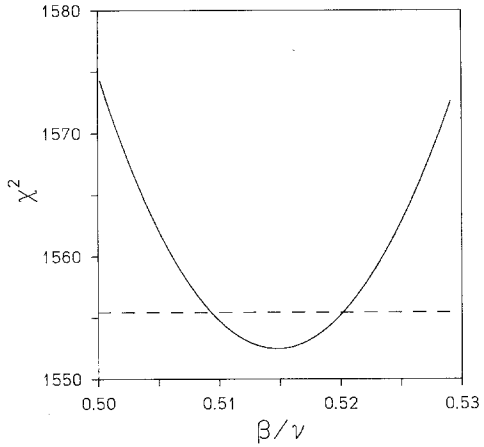

Fig. 5. Plot of χ^2 for Fit C to the data in Fig. 3 as a function of β/ν. The broken line indicates an increase $\Delta\chi^2 = 3$ over the maximum value.

$z \neq 0$ observed in Fig. 2 is slightly more complicated. First we need to know ν in order to have a constant $z = |\tau|^{\nu} L$, and second, different combinations of exponents enter in y' and θ_1. If we fix ν at the value (39), we can scale the argument in the fit to $L = 28$ (Fit B) by $x \to x(28/L)^{\beta/\nu}$ and calculate $\chi^2(\beta)$ at $L = 36$ as a function of β. From the minimum of $\chi^2(\beta)$ displayed in Fig. 6 and $\Delta^2\chi = t_a \sim 3$, we obtain the best scaling value β,

$$\beta = 0.326(2) \tag{43}$$

compatible with the previous determination (40). Scaling down to $L = 20$, χ^2 has only a very broad minimum compatible with (40).

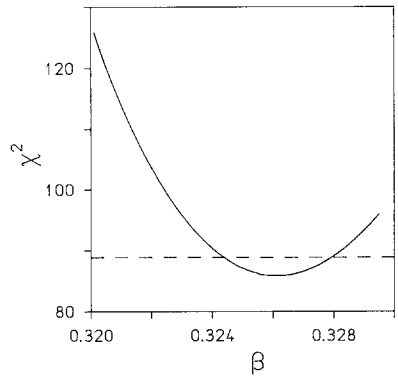

Fig. 6. Plot of χ^2 for the data at $L = 36$ in Fig. 2 scaling the Fit B to $L = 28$ by $x \to x(28/36)^{\beta/\nu}$ as a function of β for fixed $\nu = 0.629$. The broken line indicates $\Delta\chi^2 = 3$.

In the broken phase $T < T_c$ the Gaussian peak is clearly separated (see Fig. 7) and becomes more symmetric with increasing $|\tau|$. The curve in Fig. 7 represents a fit using the parametrization (35). Parameters are given in Table I (Fit E).

The determination of the critical indices is fairly accurate. With regard to the small lattice size ($L \leqslant 36$), we have to worry about corrections to scaling. A first source of scaling corrections occurs if the quantity studied receives contributions from small clusters, where the assumed scaling law (29) cannot be valid. In he analysis of critical indices we have eliminated this source by removing clusters with $s < 15$ from the fit. The more serious second source is the possibility that the asymptotic scaling equation (29) is not yet valid. In the parametrization equation (35) we can look for possible scaling violations by fitting the $\tau = 0$ data at each L separately. If scaling holds, the parameter r and the ratios σ/μ and c_p/μ should be independent of L, whereas μ should vary with L according to

$$\mu = \mu(L_0)(L/L_0)^{-\beta/\nu} \tag{44}$$

The resulting values of μ are shown in Fig. 8 as a function of L. The power law (44) is well satisfied with an exponent

$$\beta/\nu = 0.511(4) \tag{45}$$

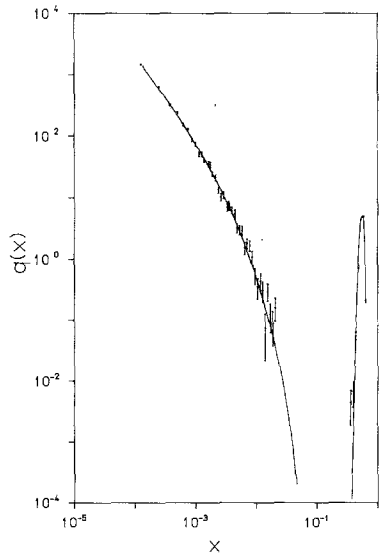

Fig. 7. Cluster distribution q for $T < T_c$ at $\tau = 0.023$ and $L = 20$ ($z = 1.86$) as a function of x on a double log scale. The curve is a fit using parametrization (35) with parameters given in Table I, Fit E.

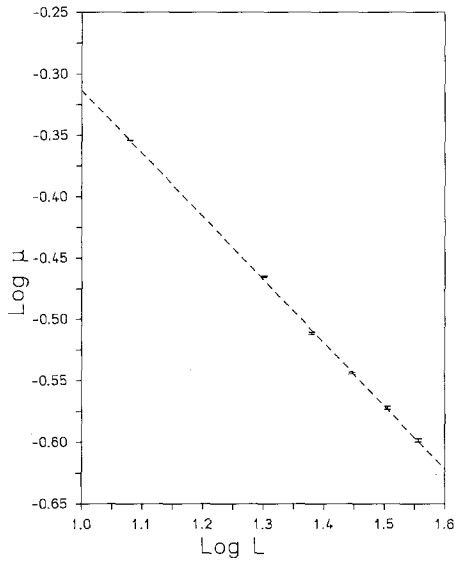

Fig. 8. Fitted values of μ at $\tau = 0$ using (35) as a function of L on a double log scale. The straight broken line corresponds to the power law (44) with $\beta/\nu = 0.511(3)$. Errors of the fit values of μ are scaled by $t_A = 3$.

which agrees with our determination (42). The other parameters (listed in Table II) are compatible with scaling. Within the validity of our parametrization we find no significant scaling violation. There remains an unknown systematic error due to the possibility that cluster distributions at $L \gg 36$ change their qualitative behavior and cannot be described by (35) or (37) with an acceptable χ^2 probability.

Table II. Values of the Parameters Describing the Percolating Clusters in Fits to the Distributions at $\tau = 0$ and Various Lattice Sizes L[a]

L	μ	σ/μ	r	c_P/μ
12	0.442(2)	0.243(1)	0.420(6)	1.84(1)
20	0.343(1)	0.251(4)	0.421(12)	1.80(1)
24	0.308(1)	0.234(8)	0.346(24)	1.77(3)
28	0.286(1)	0.255(8)	0.384(24)	1.85(3)
32	0.268(1)	0.238(10)	0.326(24)	1.69(4)
36	0.252(1)	0.240(10)	0.316(24)	1.78(4)

[a] Scaling requires σ/μ, r, and c_P/μ to be independent of L. Errors do not include t_a.

5. CONCLUSIONS

We generalized the results of de Meo *et al.*[5] about the scaling properties of SWA clusters also for the single clusters of WA. For the $d=3$ Ising model these scaling properties were well satisfied by the data. We found that the cluster distributions can be fitted with relatively simple functions. This parametrization allows the determination of the critical exponent $\beta/\nu = 0.516(6)$ from finite-size scaling at $r=0$. To derive the value $\beta = 0.326(2)$ from scaling at $z \neq 0$, a value of $\nu = 0.629$ had to be used. The exponent θ_1 in the parametrization of $q(x)$ distributions (8) at one value of T and L turned out to differ significantly from $1/\delta$ if data for low cluster sizes $s \leqslant 15$ are included. Omitting the latter, we find that θ_1 is compatible with $1/\delta$; however, the fitted value strongly depends on the details of the parametrization. The same effect has been observed in $d=2$.[5]

In our parametrization finite-size effects are described by an asymmetric Gaussian, leading to a suprisingly good descrition of the distribution of the transition region from the power law to the sharp drop induced by the finite size L. The parameter describing the Gaussian peak exhibits the L dependence expected from finite-size scaling. Given the parametrization, we do not see any scale violations within our statistics. Using cylinder geometry, we checked that the largest clusters are indeed the clusters percolating in the finite volume.

ACKNOWLEDGMENTS

We thank Dr. U. Wolff for stimulating discussions and Prof. Dr. K. Binder for sending us a copy of ref. 5 prior to publication.

REFERENCES

1. K. Binder, *Phase Transitions and Critical Phenomena*, Vol. 5b, C. Domb and M. S. Green, eds. (Academic Press, London, 1976).
2. A. D. Sokal, Monte Carlo methods in statistical physics: Foundations and new algorithms, Lecture Notes of the Cours de Troisième cycle de la Physique en Suisse Romande, Lausanne (1989).
3. R. H. Swendsen and J. S. Wang, *Phys. Rev. Lett.* **58**:86 (1987).
4. U. Wolff, *Phys. Rev. Lett.* **62**:361 (1989).
5. M. D. de Meo, D. W. Heermann, and K. Binder, *J. Stat. Phys.* **60**:585 (1990).
6. P. Tamayo, R. C. Brower, and W. Klein, *J. Stat. Phys.* **58**:1083 (1990).
7. U. Wolff, *Phys. Lett. B* **228**:361 (1989).
8. P. D. Coddington and C. F. Baillie, in *Application of Transputers: 2. Proceeding of the Second International Conference on Application of Transputers* (Southampton, U.K., 1990), p. 488.
9. A. Coniglio and W. Klein, *J. Phys. A* **13**:2775 (1980).

10. C.-K. Hu, *Phys. Rev. B* **29**:5103 (1984).
11. C. M. Fortuin and P. W. Kasteleyn, *Physica* **57**:536 (1972); C. M. Fortuin, *Physics* **58**:393 (1972).
12. U. Wolff, Critical slowing down, Bielefeld reprint BI-TP 89/35, to appear in the proceedings of LATTICE'89 Capri, Italy.
13. D. Stauffer, *Introduction to Percolation Theory* (Taylor and Francis, London, 1985); M. E. Fisher, *Physics* **3**:267 (1967).
14. M. E. Fisher and M. N. Barber, *Phys. Rev. Lett.* **28**:1516 (1972).
15. H. Kunz and B. Souillard, *J. Stat. Phys.* **19**:77 (1978).
16. M. E. Fisher, *Physics* **3**:255 (1967).
17. G. S. Pawley, R. H. Swendsen, D. J. Wallace, and K. G. Wilson, *Phys. Rev. B* **29**:4030 (1984).
18. R. B. Pearson, J. L. Richardson, and D. Toussaint, *J. Comput. Phys.* **51**:241 (1983).
19. M. N. Barber, R. B. Pearson, D. Toussaint, and J. L. Richardon, *Phys. Rev. B* **32**:1720 (1985).
20. S. Adler, *J. Phys. A* **16**:3585 (1983).